

LLM4Mat-Bench: Benchmarking Large Language Models for Materials Property Prediction

Andre Niyongabo Rubungo^{1,2}, Kangming Li³, Jason Hattrick-Simpers^{3,4,5,6},
and
Adji Bousso Dieng^{1,2,*}

¹Department of Computer Science, Princeton University

²Vertaix

³Acceleration Consortium, University of Toronto

⁴Department of Materials Science and Engineering, University of Toronto

⁵Vector Institute for Artificial Intelligence

⁶Schwartz Reisman Institute for Technology and Society

*Corresponding author: adji@princeton.edu

November 11, 2024

Abstract

Large language models (LLMs) are increasingly being used in materials science. However, little attention has been given to benchmarking and standardized evaluation for LLM-based materials property prediction, which hinders progress. We present LLM4Mat-Bench, the largest benchmark to date for evaluating the performance of LLMs in predicting the properties of crystalline materials. LLM4Mat-Bench contains about 1.9M crystal structures in total, collected from 10 publicly available materials data sources, and 45 distinct properties. LLM4Mat-Bench features different input modalities: crystal composition, CIF, and crystal text description, with 4.7M, 615.5M, and 3.1B tokens in total for each modality, respectively. We use LLM4Mat-Bench to fine-tune models with different sizes, including LLM-Prop and MatBERT, and provide zero-shot and few-shot prompts to evaluate the property prediction capabilities of LLM-chat-like models, including Llama, Gemma, and Mistral. The results highlight the challenges of general-purpose LLMs in materials science and the need for task-specific predictive models and task-specific instruction-tuned LLMs in materials property prediction ¹.

Keywords: large language models, materials property prediction, crystalline materials, benchmarks

1 Introduction

With the remarkable success of large language models (LLMs) in solving natural language tasks (Devlin et al., 2018; Radford et al., 2018; Raffel et al., 2020; Achiam et al., 2023; Touvron et al., 2023) and different scientific tasks (Lin et al., 2022;

¹The Benchmark and code can be found at: <https://github.com/vertaix/LLM4Mat-Bench>

Edwards et al., 2022; Valentini et al., 2023; Castro Nascimento and Pimentel, 2023; Fang et al., 2023; Lv et al., 2024), scientists have recently started to leverage LLMs to tackle very important and challenging problems in materials science, including predicting materials properties (Rubungo et al., 2023; Korolev and Protsenko, 2023; Xie et al., 2023; Das et al., 2023; Qu et al., 2024; Choudhary, 2024) and discovering new materials (Antunes et al., 2023; Gruver et al., 2023; Qu et al., 2024; Choudhary, 2024).

The learning capabilities of LLMs have the potential to revolutionize the field of materials science. For example, recent research by Rubungo et al. (2023) has demonstrated the exceptional performance of LLMs in predicting the properties of crystalline materials based on textual descriptions of their structures. In their study, they introduced a novel dataset, TextEdge, which comprises textual descriptions of crystals and their corresponding properties. This dataset was used to fine-tune the encoder component of the T5-small model for the task of materials property prediction. The findings of Rubungo et al. (2023) challenge the conventional practice of heavily relying on graph neural networks and using solely either crystal composition or structure as input for property prediction. Their work underscores the significance of further investigating the extent to which LLMs can be harnessed to develop innovative techniques for accurately predicting the properties of crystalline materials, thereby enhancing the materials discovery pipeline. Unfortunately, the proposed TextEdge dataset is limited in scope, comprising approximately 145K samples and encompassing only three distinct properties. Furthermore, its lack of diversity, being derived from a single data source (Materials Project (Jain et al., 2013)), hinders its effectiveness in assessing the robustness of LLMs in materials property prediction.

In this work, we introduce LLM4Mat-Bench, a benchmark dataset collected to evaluate the performance of LLMs in predicting the properties of crystalline materials. To the best of our knowledge, LLM4Mat-Bench is the most extensive benchmark to date for assessing the efficacy of language models in materials property prediction. The dataset comprises approximately two million samples, sourced from ten publicly available materials sources, each containing between 10K and 1M structure samples. LLM4Mat-Bench encompasses several tasks, including the prediction of electronic, elastic, and thermodynamic properties based on a material’s composition, crystal information file (CIF), or textual description of its structure. We use LLM4Mat-Bench to evaluate several LLMs of different sizes, namely LLM-Prop (Rubungo et al., 2023) (35M parameters), MatBERT (Walker et al., 2021) (109.5M parameters), and Llama2 (Touvron et al., 2023) (7B parameters). And we provide fixed train-valid-test splits, along with carefully designed zero-shot and few-shot prompts to ensure reproducibility. We anticipate that LLM4Mat-Bench will significantly advance the application of LLMs in addressing critical challenges in materials science, including property prediction and materials discovery.

2 LLM4Mat-Bench

2.1 Data Collection Process

We collected the data used to create LLM4Mat-Bench from 10 publicly available materials data sources. In this section, we describe each data source and discuss how we accessed its data.

2.1.1 Data sources

hMOF (Wilmer et al., 2012) is a publicly available database² consisting of about 160K Metal-Organic Frameworks (MOFs), generated by Wilmer et al. using computational approaches. Materials Project (MP) (Jain et al., 2013) is a database with around 150K materials, offering free API access³ for data retrieval, including CIF files and material properties. The Open Quantum Materials Database (OQMD) (Kirklin et al., 2015) is a publicly accessible database⁴ of 1.2M materials, containing DFT-calculated thermodynamic and structural properties, created at Northwestern University. OMDB (Borysov et al., 2017) is an organic materials database with about 12K structures and related electronic band structure properties, freely available⁵. JARVIS-DFT (Choudhary et al., 2017, 2018) is a repository created by NIST researchers, containing around 75.9K material structures with downloadable properties⁶. QMOF (Rosen et al., 2021, 2022) is a quantum-chemical property database of over 16K MOFs, accessible via GitHub⁷. JARVIS-QETB (Garrity and Choudhary, 2023) is a NIST-created database⁸ of nearly one million materials with tight-binding parameters for 65 elements. GNoME is a database of 381K new stable materials discovered by Merchant et al. (2023) using graph networks and DFT, available on GitHub⁹. Cantor HEA (Li et al., 2024) is a DFT dataset of formation energies for 84K alloy structures, available on Zenodo¹⁰. SNUMAT is a database with around 10K experimentally synthesized materials and DFT properties, accessible via API¹¹.

2.1.2 Collecting crystal information files (CIFs) and materials property

Crystal structure files (CIFs), material compositions, and material properties were collected from publicly accessible sources described in Section 2.1.1. Data collection was facilitated by APIs and direct download links provided by the respective databases. For databases such as Materials Project, OMDB, SNUMAT, JARVIS-DFT, and JARVIS-QETB, user registration is required for access, while databases like hMOF, QMOF, OQMD, and GNoME allow direct data access without registration. From each source, we obtained CIFs and associated material properties. Although

²<https://mof.tech.northwestern.edu/>

³<https://next-gen.materialsproject.org/api>

⁴<https://www.oqmd.org/>

⁵<https://omdb.mathub.io/>

⁶<https://jarvis.nist.gov/jarvisdft>

⁷<https://github.com/Andrew-S-Rosen/QMOF>

⁸<https://jarvis.nist.gov/jarvisqetb/>

⁹https://github.com/google-deepmind/materials_discovery/blob/main/DATASET.md

¹⁰<https://doi.org/10.5281/zenodo.10854500>

¹¹<https://www.snumat.com/apis>

the Materials Project and JARVIS-DFT databases offer a broader range of properties, we selected a subset—10 and 20 properties respectively—that adequately represents the data within our benchmark, based on the number of data points available for each property. This selection was made to optimize computational efficiency when training models across the 65 properties included in LLM4Mat-Bench.

2.1.3 Generating the textual description of crystal structure

LLMs perform better with textual input, and Rubungo et al. (2023); Korolev and Protsenko (2023); Qu et al. (2024) have demonstrated that LLMs can effectively learn the structural representation of a crystal from its textual description, outperforming graph neural network (GNN)-based models that directly utilize the crystal structure for property prediction.

Crystal structures are typically described in file formats such as Crystallographic Information File (CIF) which include predominantly numbers describing lattice vectors and atomic coordinates and are less amenable to LLMs. Instead of directly using these as inputs, we use Robocrystallographer (Jain et al., 2013) to deterministically generate texts that are more descriptive of crystal structures from CIF files. Robocrystallographer was developed and has been used by the Materials Project team to auto-generate texts for their database. Given a structure, Robocrystallographer leverages predefined rules and existing libraries to extract chemical and structural information, including oxidation states, global structural descriptions (symmetry information, prototype matching, structural fingerprint calculations etc.), and local structural descriptions (e.g. bonding and neighbor analysis, connectivity). This method not only generate deterministic and human-readable texts, but also ensures no data contamination in our fine-tuned LLMs, as the data sources mentioned do not include these crystal text descriptions.

Table 1: LLM4Mat-Bench statistics.

Data source	# Structure files	# Structure-Description pairs				# Tokens (Words)			# Avg. subword tokens/Sample			# Properties
		Total	Train	Validation	Test	Composition	Structure	Description	Composition	Structure	Description	
QCMD (Kirkin et al., 2015)	1,008,266	964,403	771,522	96,440	96,441	964K	96M	244M	5.3	635.4	347.3	2
JARVIS-QETB (Garrity and Choudhary, 2023)	829,576	623,989	499,191	62,399	62,399	624K	45M	90M	3.5	466.6	202.5	4
GNoME (Merchani et al., 2023)	381,000	376,276	301,020	37,628	37,628	830K	78M	508M	9.7	1185.3	1711.3	6
Materials Project (Jain et al., 2013)	146,143	146,143	125,825	10,000	10,318	272K	37M	157M	6.8	1611.8	1467.3	10
hMOF (Wilmer et al., 2012)	133,524	132,743	106,194	13,274	13,275	449K	96M	581M	14.9	4583.9	5629.3	7
Cantor HEA (Li et al., 2024)	84,024	84,019	67,215	8,402	8,402	84K	11M	251M	9.5	868.4	4988.6	4
JARVIS-DFT (Choudhary et al., 2017, 2018)	75,965	75,965	60,772	7,596	7,597	76K	9M	25M	5.0	786.0	455.9	20
QMOP (Rosen et al., 2021, 2022)	16,340	7,656	6,124	766	766	8K	7M	22M	14.0	5876.4	3668.0	4
OMDB (Borysov et al., 2021, 2022)	12,500	12,122	9,697	1,212	1,213	66K	8M	14M	14.8	4097.4	1496.6	1
SNUMAT ¹²	10,481	10,372	8,297	1,037	1,038	16K	2M	4M	5.9	1244.5	539.1	7
Total	2,697,779	1,978,985	1,592,315	193,357	193,313	4.7M	615.5M	3.1B	7.9	1559.7	1703.6	65

Table 2: Comparing the LLM4Mat-Bench with other existing benchmarks.

Benchmark	# Data Sources	# Distinct Properties	# Properties/# Samples			# Properties/Task Type		Material Representations		
			<10k	10-100k	100k+	Regression	Classification	Composition	Structure	Description
MatBench (Dunn et al., 2020)	6	10	7	3	3	10	3	✓	✓	✓
TextEdge (Rubungo et al., 2023)	1	3	0	0	3	2	1	✗	✗	✓
LLM4Mat-Bench (Ours)	10	45	5	31	29	60	5	✓	✓	✓

2.2 Data Statistics

As Table 1 shows, LLM4Mat-Bench comprises 2,697,779 structure files, which, after pairing with descriptions generated by Robocrystallographer and filtering out descriptions with fewer than five words, result in 1,978,985 composition-structure-

description pairs¹³. The reduction in sample count is also due to Robocrystallographer’s inability to describe certain CIF files. The total samples for each dataset in LLM4Mat-Bench are randomly split into 80%, 10%, and 10% for training, validation, and testing, respectively. OQMD has the highest number of samples at 964,403, while QMOF has the fewest with 7,656 samples. On average, each dataset in LLM4Mat-Bench contains approximately 200,000 samples.

In LLM4Mat-Bench, when combined, textual descriptions contain 3.1 billion tokens, crystal structures 615 million, and compositions 4.7 million¹⁴. OQMD leads in composition tokens (964K), while hMOF has the most description tokens (581M). For CIFs, both OQMD and hMOF have around 96M tokens. On average, compositions have 8 subword tokens per sample, CIFs 1600, and descriptions 1700. hMOF averages the longest inputs for compositions (14.9) and descriptions (5629), while QMOF leads in structures (5876.4)¹⁵. JARVIS-DFT has the most tasks with 20 properties, followed by Materials Project with 10, and OMDB with one. Details on sample counts are in Section 3.2.

LLM4Mat-Bench provides the most comprehensive dataset compared to existing benchmarks, with the largest number of samples, properties, and tasks, including 60 regression and 5 classification tasks (see Table 2). It also offers more diverse material representations, incorporating chemical formulas, crystal structures, and crystal text descriptions. In contrast, MatBench (Dunn et al., 2020) and TextEdge (Rubungo et al., 2023) have fewer tasks and less representation diversity, with MatBench lacking crystal text descriptions and TextEdge missing material compositions and crystal structures.

2.3 Data Quality

Since Robocrystallographer generates crystal text descriptions in a deterministic manner following predefined and well-validated rules (Jain et al., 2013), these texts should faithfully describe the crystal structures used to generate them. Regarding the quality of labels, they are calculated from simulations and are usually considered noise-free. Properties data except those from JARVIS-QETB and hMOF are obtained from DFT, which is based on fundamental quantum mechanical equations. While DFT calculations can still be performed with different levels of approximations and fidelity, the DFT-calculated properties are usually considered to be highly reliable and are routinely used as noise-free ground truths for ML models in the materials science community.

3 Results

3.1 Experimental Details

We conducted about 845 experiments, evaluating the performance of five models and three material representations on each property for each data source. Consistent

¹³The total number of pairs were 2,433,688, after removing about 454703 duplicated pairs across datasets, it resulted to 1,978,985 pairs.

¹⁴We used NLTK toolkit as a tokenizer to count the number of words/tokens.

¹⁵We used Llama 2 tokenizer to count the number of subword tokens.

with standard practices in materials science, we evaluated performance separately for each data source rather than combining samples from different sources for the same property. This approach accounts for variations in techniques and settings used by different data sources, which can result in discrepancies, such as differing band gaps for the same material. Below, we will describe each material representation, model, and metric that we used to conduct our experiments.

3.1.1 Material Representations

LLM4Mat-Bench includes three distinct materials representations: Composition, CIF, and Description (see Table 6). The primary goal of using these diverse representations is to identify which best enhances LLM performance in predicting material properties across different data sources.

Composition (Comp.) Material composition refers to the chemical formula of a material. Though it only provides stoichiometric information, studies have shown it can still be a reliable material representation for property prediction (Dunn et al., 2020; Tian et al., 2022). For LLMs, it offers the advantage of being a short sequence that usually fits within the model’s context window, making it efficient to train. To further optimize efficiency, we set the longest sequence of material compositions from each data source as the context window, rather than using the default 512 tokens for fine-tuning while the original length is kept during inference.

CIF We represent the materials structure using CIF files, the conventional way of representing the crystal structure in crystallography (Hall et al., 1991). CIFs are commonly used for GNN-based models, but some recent works have demonstrated that it can also work with LLMs (Antunes et al., 2023; Flam-Shepherd and Aspuru-Guzik, 2023; Gruver et al., 2023).

Description (Descr.) As we outlined in Section 2.1.3, we also use textual descriptions of crystal structures as representations for both atomic crystals and MOFs.

3.1.2 Models

We benchmarked different LLM-based models with various sizes, and a GNN-based baseline. Herein, We provide the details of each model.

CGCNN (Xie and Grossman, 2018) is employed as a GNN baseline which is widely used in the materials science community¹⁶. We trained on LLM4Mat-Bench from scratch with optimal hyperparameters: 128 hidden dimensions, batch size of 256, three message passing layers, 1e-2 learning rate, 8.0 radius cutoff, 12 nearest neighbors, and 500 training epochs, though extending to 1000 epochs improved performance in some cases.

MatBERT (Walker et al., 2021) is a BERT-base model (Devlin et al., 2018) with 109 million parameters, pretrained on two million materials science articles. We

¹⁶Although CGCNN is not state-of-the-art for some properties, it was faster compared to models like ALIGNN (Choudhary and DeCost, 2021) and DeeperGatGNN (Omeel et al., 2022), making it suitable for our extensive experiments

property prediction, we tested Llama 2-7b-chat (7 billion parameters) using our designed zero-shot and five-shot prompts (see Table 3) without fine-tuning. For the CIF structure prompts, we removed "# generated using pymatgen" comment that is appended to each file. The maximum input length was set to 4000 tokens while the output length was set to 256, with a batch size of 256 samples, temperature of 0.8, and top-K sampling applied with $K = 10$. The details of other models that we compared with Llama 2 can be found in Appendix C. For five-shot examples, we sampled from crystals with shorter structures and descriptions to reduce the context length. We also made sure the property values for those examples are diverse (for instance, they should not all have 0.0 eV as their bandgap values).

We trained all models using NVIDIA RTX A6000 GPUs. Training MatBERT with two GPUs on about 300K data points and 100 epochs took about four days while for LLM-Prop took about 2.5 days. For CGCNN, it took about 7 hours training time on one GPU for 500 epochs. With one GPU, Llama 2 took about a half day to generate the output of 40K samples with 256 tokens maximum length each. We report the test set results averaged over five runs for predictive models and three runs for generative models.

3.1.3 Evaluation Metrics

Following Choudhary and DeCost (2021), we evaluated regression tasks using the ratio between the mean absolute deviation (MAD) of the ground truth and the mean absolute error (MAE) of the predicted properties. The MAD:MAE ratio ensures an unbiased model comparison between different properties where the higher ratio the better. According to Choudhary and DeCost (2021), a good predictive model should have at least 5.0 ratio. MAD values represent the performance of a random guessing model predicting the average value for each data point. To provide a comprehensive performance comparison across datasets, we also reported the weighted average of MAD:MAE across all properties in each dataset (Wtd. Avg. (MAD:MAE), see Equation 1).

For classification tasks, we reported the area under the ROC curve (AUC) for each task and provided the weighted average across all properties (Wtd. Avg. AUC, see Equation 2).

$$\text{Wtd. Avg. (MAD/MAE)} = \frac{\sum_i^m \text{TestSize}_i \times \frac{\text{MAD}_i}{\text{MAE}_i}}{\sum_i^m \text{TestSize}_i}, \quad (1)$$

$$\text{Wtd. Avg. AUC} = \frac{\sum_i^m \text{TestSize}_i \times \text{AUC}_i}{\sum_i^m \text{TestSize}_i}, \quad (2)$$

m denotes the number of regression properties in the dataset.

3.2 Discussion

Table 4 and 5, and Figure 1 and 2 show the main results. The detailed results on each dataset can be found in Appendix E. The main observations are as follows:

Table 4: The Wtd. Avg. (MAD/MAE) scores (the higher the better) for the regression tasks in the LLM4Mat-Bench are reported. **Bolded** results indicate the best model for each input format, while **bolded results with blue background** highlight the best model per each dataset. **Inval.** denotes cases where the Llama model failed to generate outputs with a property value or had fewer than 10 valid predictions.

Input	Model	Dataset									
		MP 8 tasks	JARVIS-DFT 20 tasks	GNoME 6 tasks	hMOF 7 tasks	Cantor HEA 4 tasks	JARVIS-QETB 4 tasks	OQMD 2 tasks	QMOF 4 tasks	SNUMAT 4 tasks	OMDB 1 task
CIF	CGCNN (baseline)	5.319	7.048	19.478	2.257	17.780	61.729	14.496	3.076	1.973	2.751
Comp.	Llama 2-7b-chat:0S	0.389	Inval.	0.164	0.174	0.034	0.188	0.105	0.303	0.940	0.885
	Llama 2-7b-chat:5S	0.627	0.704	0.499	0.655	0.867	1.047	1.160	0.932	1.157	1.009
	MatBERT-109M	5.317	4.103	12.834	1.430	6.769	11.952	5.772	2.049	1.828	1.554
	LLM-Prop-35M	4.394	2.912	15.599	1.479	8.400	59.443	6.020	1.958	1.509	1.507
CIF	Llama 2-7b-chat:0S	0.392	0.216	6.746	0.214	0.022	0.278	0.028	0.119	0.682	0.159
	Llama 2-7b-chat:5S	Inval.	Inval.	Inval.	Inval.	Inval.	1.152	1.391	Inval.	Inval.	0.930
	MatBERT-109M	7.452	6.211	14.227	1.514	9.958	47.687	10.521	3.024	2.131	1.777
	LLM-Prop-35M	8.554	6.756	16.032	1.623	15.728	97.919	11.041	3.076	1.829	1.777
Descr.	Llama 2-7b-chat:0S	0.437	0.247	0.336	0.193	0.069	0.264	0.106	0.152	0.883	0.155
	Llama 2-7b-chat:5S	0.635	0.703	0.470	0.653	0.820	0.980	1.230	0.946	1.040	1.001
	MatBERT-109M	7.651	6.083	15.558	1.558	9.976	46.586	11.027	3.055	2.152	1.847
	LLM-Prop-35M	9.116	7.204	16.224	1.706	15.926	93.001	9.995	3.016	1.950	1.656

Table 5: The Wtd. Avg. AUC scores (the higher the better) for the classification tasks in the LLM4Mat-Bench.

Input	Model	Dataset	
		MP 2 tasks	SNUMAT 3 tasks
CIF	CGCNN (baseline)	0.846	0.722
Comp.	Llama 2-7b-chat:0S	0.491	Inval.
	Llama 2-7b-chat:5S	0.507	0.466
	MatBERT-109M	0.722	0.712
	LLM-Prop-35M	0.691	0.716
CIF	Llama 2-7b-chat:0S	0.501	0.489
	Llama 2-7b-chat:5S	0.502	0.474
	MatBERT-109M	0.750	0.717
	LLM-Prop-35M	0.738	0.660
Descr.	Llama 2-7b-chat:0S	0.500	Inval.
	Llama 2-7b-chat:5S	0.502	0.568
	MatBERT-109M	0.735	0.730
	LLM-Prop-35M	0.742	0.735

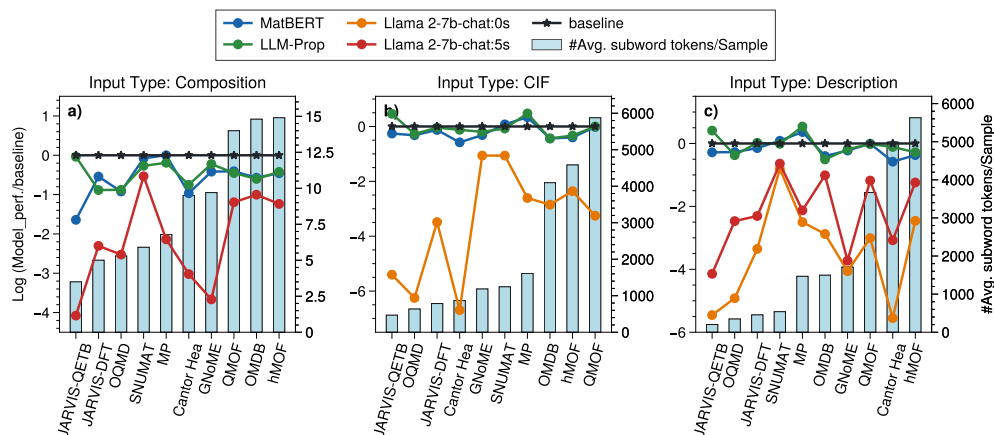


Figure 1: The performance comparison across models for each material representation is presented. The left y-axis shows the log-normalized performance of each LLM-based model relative to the baseline (CGCNN), while the right y-axis (bar plots) displays the average subword tokens per sample for each dataset. Datasets on the x-axis are ordered by increasing average subword tokens. Results for Llama 2-7b-chat:0S and Llama 2-7b-chat:5S are missing in plots (a) and (b), respectively, due to invalid outputs. Higher values in the line plots indicate better performance.

Small, task-specific predictive LLMs exhibit significantly better performance than larger, generative general-purpose LLMs. This performance disparity is evident across both regression (Table 4 and Figure 1) and classification tasks (Table 5) on all 10 datasets. Specifically, LLM-Prop and MatBERT outperform Llama 2-7b-chat:0S and Llama 2-7b-chat:5S by a substantial margin, despite being approximately 200 and 64 times smaller in size, respectively. In regression tasks, LLM-Prop achieves the highest accuracy on 8 out of 10 datasets, with MatBERT leading on the remaining 2 datasets. For classification tasks, both LLM-Prop and MatBERT deliver the best performance on 1 out of 2 datasets. LLM-Prop surpasses MatBERT by 1.8% on the SNUMAT dataset, whereas MatBERT outperforms LLM-Prop by 0.8% on the other dataset. As anticipated, a modest enhancement in average performance is observed across various datasets and input formats when the Llama 2-7b-chat model is evaluated using 5-shot prompts rather than 0-shot prompts. Determining the optimal number of examples required to achieve peak performance will be the focus of future work.

General-purpose generative LLMs hallucinate and often fail to generate valid property values. As shown in Table 4, Table 5, Figure 2, and Appendix E, Llama 2-7b-chat model produces invalid outputs on multiple tasks, where the expected property value is missing. This issue occurs less frequently when the input is a description or chemical formula, but more commonly when the input is a CIF file. One reason may be that descriptions and chemical formulas resemble natural language, which LLMs can more easily interpret compared to CIF files. This may also indicate that when the input modality during inference differs significantly from the modalities encountered during pretraining, fine-tuning is necessary to achieve reasonable performance. Another key observation is that Llama 2-7b-chat model often generates the same property value for different inputs (i.e. hallucinates),

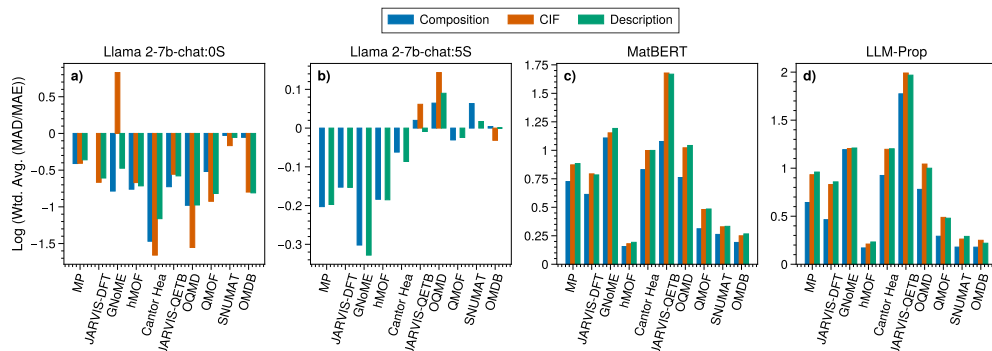


Figure 2: The performance comparison across material representations for each LLM-based model is shown. The y-axis represents the log-normalized Weighted Average (MAD/MAE) score for each representation, while the x-axis displays randomly ordered datasets. In the (a) and (b) plots, some Composition and Structure performance results are missing due to invalid outputs. A higher y-axis value indicates better performance.

contributing to its poor performance across multiple tasks. These findings highlight the importance of caution when using general-purpose generative LLMs for materials property prediction and emphasize the need for fine-tuned, task-specific LLM-based models.

Representing materials with their textual descriptions improves the performance of LLM-based property predictors compared to other representations. We observe a significant performance improvement when the input is a description compared to when it is a CIF file or a chemical formula. One of the possible reasons for this might be that LLMs are more adept at learning from natural language data. On the other hand, although material compositions appear more natural to LLMs compared to CIF files, they lack sufficient structural information. This is likely why LLMs with CIF files as input significantly outperform those using chemical formulas.

More advanced, general-purpose generative LLMs do not necessarily yield better results in predicting material properties. In Figure 3, we compare the performance of Llama 2-7b-chat-hf model with advanced versions of Llama of comparable sizes when predicting material’s band gap and its stability. Similar comparisons are also conducted for the Mistral (Jiang et al., 2023) and Gemma (Team et al., 2024) models. The results indicate that, despite being trained on substantially larger and higher-quality datasets, more advanced versions of generative LLMs show limited improvements in performance and validity of predictions for material properties. For instance, Llama 3 and 3.1 8b models were trained on over 15 trillion tokens—around eight times more data than the 2 trillion tokens used for the Llama 2 7b models. This finding highlights the ongoing challenges of leveraging LLMs in material property prediction and underscores the need for further research to harness the potential of these robust models in this domain.

The performance on energetic properties is consistently better across all datasets compared to other properties. This is consistent with the trend observed

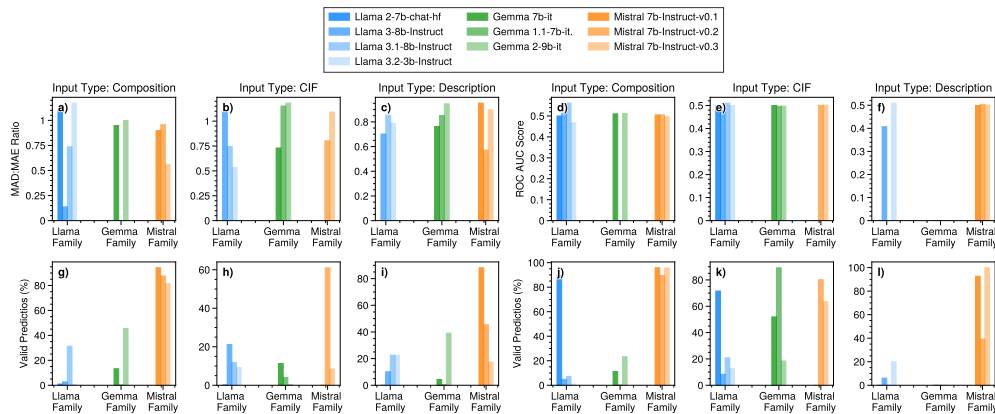


Figure 3: The performance comparison of different chat-based LLM versions is presented with results based on 5-shot prompts, averaged over three inference runs. Panels (a)–(c) and (d)–(f) show each model’s accuracy in predicting band gaps and stability in the MP dataset, respectively, while panels (g)–(i) and (j)–(l) depict the percentage of valid predictions for band gap and stability on the test set.

in the community benchmarks such as MatBench and JARVIS-Leaderboard, where energetic properties are among those that can be most accurately predicted (Dunn et al., 2020; Choudhary et al., 2024). This is not surprising because energy is known to be relatively well predicted from e.g., compositions and atom coordination (bonding), which is inherently represented in GNNs and also presented in text descriptions.

Task-specific predictive LLM-based models excel with shorter textual descriptions, while CGCNN performs better on datasets with longer descriptions. While the focus on this work is on LLMs, a comparison with a simple but widely used GNN-based baseline suggests room for improvement in LLM-based property prediction. For regression tasks, LLM-Prop outperforms CGCNN on only 4 out of 10 datasets (MP, JARVIS-DFT, JARVIS-QETB, and SNUMAT), and MatBERT outperforms CGCNN on just 2 out of 10 datasets (MP and JARVIS-QETB). In contrast, CGCNN achieves the best performance on 5 out of 10 datasets (GNoME, hMOF, Cantor HEA, OQMD, and OMDB). Further analysis reveals that CGCNN tends to perform better than LLM-based models on datasets with relatively longer textual descriptions, while LLM-based models excel on datasets with shorter descriptions (see Table 1). The performance gain on shorter descriptions may stem from LLM-based models’ ability to leverage more context from compact text, while CGCNN consistently benefits from training on the entire crystal structure.

4 Conclusion

LLMs are increasingly being utilized in materials science, particularly for materials property prediction and discovery. However, the absence of standardized evaluation benchmarks has impeded progress in this field. We introduced LLM4Mat-Bench, a comprehensive benchmark dataset designed to evaluate LLMs for predicting properties of atomic and molecular crystals and MOFs. Our results demonstrate

the limitations of general-purpose LLMs in this domain and underscore the necessity for task-specific predictive models and instruction-tuned LLMs tailored for materials property prediction. These findings emphasize the importance of using LLM4Mat-Bench to advance the development of more effective LLMs in materials science.

5 Limitations

Due to computational constraints and the number of experiments, we were unable to conduct thorough hyperparameter searches for each property and dataset. The reported settings were optimized on the MP dataset and then fixed for other datasets. For each model, we highlighted hyperparameter settings that may improve performance (see Section 3.1.2). Additionally, we could not include results from SOTA commercial LLMs such as GPT-4o¹⁷ or Claude 3.5 Sonnet¹⁸ due to budget constraints.

We also encountered issues with chat-based models, which sometimes failed to follow the output format, producing invalid or incomplete outputs. Extracting property values was therefore challenging. We believe further instruction-tuning chat-based models on the provided prompts could mitigate these issues.

Furthermore, we did not include comparisons with dataset-specific retrieval-augmented generation (RAG) models, such as the recently developed LLaMP (Chiang et al., 2024), a RAG-based model tailored for interaction with the MP dataset. Our work aims to provide a comprehensive benchmark and baseline results to advance the evaluation of LLM-based methods for materials property prediction. Future work should address these limitations.

Acknowledgments

Adji Bousso Dieng acknowledges support from the National Science Foundation, Office of Advanced Cyberinfrastructure (OAC) #2118201, and from the Schmidt Sciences AI2050 Early Career Fellowship.

References

- Achiam, J., Adler, S., Agarwal, S., Ahmad, L., Akkaya, I., Aleman, F. L., Almeida, D., Altschmidt, J., Altman, S., Anadkat, S., et al. (2023). Gpt-4 technical report. *arXiv preprint arXiv:2303.08774*.
- Antunes, L. M., Butler, K. T., and Grau-Crespo, R. (2023). Crystal structure generation with autoregressive large language modeling. *arXiv preprint arXiv:2307.04340*.
- Borysov, S. S., Geilhufe, R. M., and Balatsky, A. V. (2017). Organic materials database: An open-access online database for data mining. *PLoS one*, 12(2):e0171501.

¹⁷<https://openai.com/index/hello-gpt-4o/>

¹⁸<https://www.anthropic.com/news/claude-3-5-sonnet>

- Castro Nascimento, C. M. and Pimentel, A. S. (2023). Do large language models understand chemistry? a conversation with chatgpt. *Journal of Chemical Information and Modeling*, 63(6):1649–1655.
- Chiang, Y., Chou, C.-H., and Riebesell, J. (2024). Llamp: Large language model made powerful for high-fidelity materials knowledge retrieval and distillation. *arXiv preprint arXiv:2401.17244*.
- Choudhary, K. (2024). Atomgpt: Atomistic generative pretrained transformer for forward and inverse materials design. *The Journal of Physical Chemistry Letters*, 15(27):6909–6917.
- Choudhary, K. and DeCost, B. (2021). Atomistic line graph neural network for improved materials property predictions. *npj Computational Materials*, 7(1):1–8.
- Choudhary, K., Kalish, I., Beams, R., and Tavazza, F. (2017). High-throughput identification and characterization of two-dimensional materials using density functional theory. *Scientific reports*, 7(1):5179.
- Choudhary, K., Wines, D., Li, K., Garrity, K. F., Gupta, V., Romero, A. H., Krogel, J. T., Saritas, K., Fuhr, A., Ganesh, P., et al. (2024). Jarvis-leaderboard: a large scale benchmark of materials design methods. *npj Computational Materials*, 10(1):93.
- Choudhary, K., Zhang, Q., Reid, A. C., Chowdhury, S., Van Nguyen, N., Trautt, Z., Newrock, M. W., Congo, F. Y., and Tavazza, F. (2018). Computational screening of high-performance optoelectronic materials using optb88vdw and tb-mbj formalisms. *Scientific data*, 5(1):1–12.
- Das, K., Goyal, P., Lee, S.-C., Bhattacharjee, S., and Ganguly, N. (2023). Crysmmnet: multimodal representation for crystal property prediction. In *Uncertainty in Artificial Intelligence*, pages 507–517. PMLR.
- Devlin, J., Chang, M.-W., Lee, K., and Toutanova, K. (2018). Bert: Pre-training of deep bidirectional transformers for language understanding. *arXiv preprint arXiv:1810.04805*.
- Dunn, A., Wang, Q., Ganose, A., Dopp, D., and Jain, A. (2020). Benchmarking materials property prediction methods: the matbench test set and automatminer reference algorithm. *npj Computational Materials*, 6(1):138.
- Edwards, C., Lai, T., Ros, K., Honke, G., Cho, K., and Ji, H. (2022). Translation between molecules and natural language. In *Proceedings of the 2022 Conference on Empirical Methods in Natural Language Processing*, pages 375–413.
- Fang, Y., Liang, X., Zhang, N., Liu, K., Huang, R., Chen, Z., Fan, X., and Chen, H. (2023). Mol-instructions-a large-scale biomolecular instruction dataset for large language models. In *The Twelfth International Conference on Learning Representations*.
- Flam-Shepherd, D. and Aspuru-Guzik, A. (2023). Language models can generate molecules, materials, and protein binding sites directly in three dimensions as xyz, cif, and pdb files. *arXiv preprint arXiv:2305.05708*.

- Garrity, K. F. and Choudhary, K. (2023). Fast and accurate prediction of material properties with three-body tight-binding model for the periodic table. *Physical review materials*, 7(4):044603.
- Golkar, S., Pettee, M., Eickenberg, M., Bietti, A., Cranmer, M., Krawezik, G., Lanusse, F., McCabe, M., Ohana, R., Parker, L. H., et al. (2023). xval: A continuous number encoding for large language models. In *NeurIPS 2023 AI for Science Workshop*.
- Gruver, N., Sriram, A., Madotto, A., Wilson, A. G., Zitnick, C. L., and Ulissi, Z. W. (2023). Fine-tuned language models generate stable inorganic materials as text. In *The Twelfth International Conference on Learning Representations*.
- Hall, S. R., Allen, F. H., and Brown, I. D. (1991). The crystallographic information file (cif): a new standard archive file for crystallography. *Foundations of Crystallography*, 47(6):655–685.
- Jain, A., Ong, S., Hautier, G., Chen, W., Richards, W., Dacek, S., Cholia, S., Gunter, D., Skinner, D., Ceder, G., et al. (2013). The materials project: A materials genome approach to accelerating materials innovation. *apl materials*, 1 (1): 011002, 2013.
- Jiang, A. Q., Sablayrolles, A., Mensch, A., Bamford, C., Chaplot, D. S., Casas, D. d. l., Bressand, F., Lengyel, G., Lample, G., Saulnier, L., et al. (2023). Mistral 7b. *arXiv preprint arXiv:2310.06825*.
- Kirklin, S., Saal, J. E., Meredig, B., Thompson, A., Doak, J. W., Aykol, M., Rühl, S., and Wolverton, C. (2015). The open quantum materials database (oqmd): assessing the accuracy of dft formation energies. *npj Computational Materials*, 1(1):1–15.
- Korolev, V. and Protsenko, P. (2023). Accurate, interpretable predictions of materials properties within transformer language models. *Patterns*, 4(10).
- Li, K., Choudhary, K., DeCost, B., Greenwood, M., and Hattrick-Simpers, J. (2024). Efficient first principles based modeling via machine learning: from simple representations to high entropy materials. *Journal of Materials Chemistry A*, 12(21):12412–12422.
- Lin, Z., Akin, H., Rao, R., Hie, B., Zhu, Z., Lu, W., dos Santos Costa, A., Fazel-Zarandi, M., Sercu, T., Candido, S., et al. (2022). Language models of protein sequences at the scale of evolution enable accurate structure prediction. *BioRxiv*, 2022:500902.
- Lv, L., Lin, Z., Li, H., Liu, Y., Cui, J., Chen, C. Y.-C., Yuan, L., and Tian, Y. (2024). Pro-llama: A protein large language model for multi-task protein language processing. *arXiv preprint arXiv:2402.16445*.
- Merchant, A., Batzner, S., Schoenholz, S. S., Aykol, M., Cheon, G., and Cubuk, E. D. (2023). Scaling deep learning for materials discovery. *Nature*.
- Omeo, S. S., Louis, S.-Y., Fu, N., Wei, L., Dey, S., Dong, R., Li, Q., and Hu, J. (2022). Scalable deeper graph neural networks for high-performance materials property prediction. *Patterns*, 3(5).

- Qu, J., Xie, Y. R., Ciesielski, K. M., Porter, C. E., Toberer, E. S., and Ertekin, E. (2024). Leveraging language representation for materials exploration and discovery. *npj Computational Materials*, 10(1):58.
- Radford, A., Narasimhan, K., Salimans, T., Sutskever, I., et al. (2018). Improving language understanding by generative pre-training.
- Raffel, C., Shazeer, N., Roberts, A., Lee, K., Narang, S., Matena, M., Zhou, Y., Li, W., and Liu, P. J. (2020). Exploring the limits of transfer learning with a unified text-to-text transformer. *Journal of machine learning research*, 21(140):1–67.
- Rosen, A. S., Fung, V., Huck, P., O'Donnell, C. T., Horton, M. K., Truhlar, D. G., Persson, K. A., Notestein, J. M., and Snurr, R. Q. (2022). High-throughput predictions of metal–organic framework electronic properties: theoretical challenges, graph neural networks, and data exploration. *npj Computational Materials*, 8(1):112.
- Rosen, A. S., Iyer, S. M., Ray, D., Yao, Z., Aspuru-Guzik, A., Gagliardi, L., Notestein, J. M., and Snurr, R. Q. (2021). Machine learning the quantum-chemical properties of metal–organic frameworks for accelerated materials discovery. *Matter*, 4(5):1578–1597.
- Rubungo, A. N., Arnold, C., Rand, B. P., and Dieng, A. B. (2023). Llm-prop: Predicting physical and electronic properties of crystalline solids from their text descriptions. *arXiv preprint arXiv:2310.14029*.
- Smith, L. N. and Topin, N. (2019). Super-convergence: Very fast training of neural networks using large learning rates. In *Artificial intelligence and machine learning for multi-domain operations applications*, volume 11006, pages 369–386. SPIE.
- Team, G., Mesnard, T., Hardin, C., Dadashi, R., Bhupatiraju, S., Pathak, S., Sifre, L., Rivièrè, M., Kale, M. S., Love, J., et al. (2024). Gemma: Open models based on gemini research and technology. *arXiv preprint arXiv:2403.08295*.
- Tian, S. I. P., Walsh, A., Ren, Z., Li, Q., and Buonassisi, T. (2022). What information is necessary and sufficient to predict materials properties using machine learning? *arXiv preprint arXiv:2206.04968*.
- Touvron, H., Martin, L., Stone, K., Albert, P., Almahairi, A., Babaei, Y., Bashlykov, N., Batra, S., Bhargava, P., Bhosale, S., et al. (2023). Llama 2: Open foundation and fine-tuned chat models. *arXiv preprint arXiv:2307.09288*.
- Valentini, G., Malchiodi, D., Gliozzo, J., Mesiti, M., Soto-Gomez, M., Cabri, A., Reese, J., Casiraghi, E., and Robinson, P. N. (2023). The promises of large language models for protein design and modeling. *Frontiers in Bioinformatics*, 3.
- Walker, N., Trewartha, A., Huo, H., Lee, S., Cruse, K., Dagdelen, J., Dunn, A., Persson, K., Ceder, G., and Jain, A. (2021). The impact of domain-specific pre-training on named entity recognition tasks in materials science. *Available at SSRN 3950755*.
- Wilmer, C. E., Leaf, M., Lee, C. Y., Farha, O. K., Hauser, B. G., Hupp, J. T., and Snurr, R. Q. (2012). Large-scale screening of hypothetical metal–organic frameworks. *Nature chemistry*, 4(2):83–89.

- Xie, T. and Grossman, J. C. (2018). Crystal graph convolutional neural networks for an accurate and interpretable prediction of material properties. *Physical review letters*, 120(14):145301.
- Xie, T., Wan, Y., Huang, W., Yin, Z., Liu, Y., Wang, S., Linghu, Q., Kit, C., Grazian, C., Zhang, W., et al. (2023). Darwin series: Domain specific large language models for natural science. *arXiv preprint arXiv:2308.13565*.

Appendices

Table of Contents

A	Materials Representations	18
B	Statistics of All Properties in LLM4Mat-Bench	19
C	Chat-like Model Inference Details	19
D	Prompt Templates	20
E	Result Details for Each Dataset	22
E.1	Detailed MAD:MAE Results	22
E.2	Detailed MAE Results	27

A Materials Representations

Table 6: LLM4Mat-Bench material representations of Sodium Chloride (NaCl).

Crystal Information File (CIF)

```
1 # generated using pymatgen
2 data_NaCl
3 _symmetry_space_group_name_H-M 'P 1'
4 _cell_length_a 3.50219000
5 _cell_length_b 3.50219000
6 _cell_length_c 3.50219000
7 _cell_angle_alpha 90.00000000
8 _cell_angle_beta 90.00000000
9 _cell_angle_gamma 90.00000000
10 _symmetry_Int_Tables_number 1
11 _chemical_formula_structural NaCl
12 _chemical_formula_sum 'Na1 Cl1'
13 _cell_volume 42.95553287
14 _cell_formula_units_Z 1
15 loop_
16 _symmetry_equiv_pos_site_id
17 _symmetry_equiv_pos_as_xyz
18 1 'x, y, z'
19 loop_
20 _atom_type_symbol
21 _atom_type_oxidation_number
22 Na+ 1.0
23 Cl- -1.0
24 loop_
25 _atom_site_type_symbol
26 _atom_site_label
27 _atom_site_symmetry_multiplicity
28 _atom_site_fract_x
29 _atom_site_fract_y
30 _atom_site_fract_z
31 _atom_site_occupancy
32 Na+ Na0 1 0.00000000 0.00000000 0.00000000 1
33 Cl- Cl1 1 0.50000000 0.50000000 0.50000000 1
34
```

Description

NaCl is Tetraauricupride structured and crystallizes in the cubic $P\bar{m}3m$ space group. Na^{1+} is bonded in a body-centered cubic geometry to eight equivalent Cl^{1-} atoms. All Na-Cl bond lengths are 3.03 Å. Cl^{1-} is bonded in a body-centered cubic geometry to eight equivalent Na^{1+} atoms.

B Statistics of All Properties in LLM4Mat-Bench

Table 7: Statistics of all datasets in LLM4Mat-Bench. It is important to note that we retain the naming convention of each property from the original data source with the intent to provide the distribution of properties in each dataset.

Property	Task type	# Samples/Data source									
		JARVIS-DFT	Materials Project	SNUMAT	hMOF	GNoME	JARVIS-QETB	Cantor HEA	QMOF	OQMD	OMDB
Bandgap	Regression	-	145,302	-	-	288,209	-	-	16,340	1,007,324	12,500
Bandgap (OPT)	Regression	75,965	-	-	-	-	-	-	-	-	-
Bandgap (MBJ)	Regression	19,800	-	-	-	-	-	-	-	-	-
Bandgap GGA	Regression	-	-	10,481	-	-	-	-	-	-	-
Bandgap HSE	Regression	-	-	10,481	-	-	-	-	-	-	-
Bandgap GGA Optical	Regression	-	-	10,481	-	-	-	-	-	-	-
Bandgap HSE Optical	Regression	-	-	10,481	-	-	-	-	-	-	-
Indirect Bandgap	Regression	-	-	-	-	-	829,576	-	-	-	-
Formation Energy Per Atom (FEPA)	Regression	75,965	145,262	-	-	384,871	829,576	84,024	-	1,008,266	-
Energy Per Atom (EPA)	Regression	-	145,262	-	-	-	829,576	84,024	-	-	-
Decomposition Energy Per Atom (DEPA)	Regression	-	-	-	-	384,871	-	-	-	-	-
Energy Above Hull (Ehull)	Regression	75,965	145,262	-	-	-	-	84,024	-	-	-
Total Energy	Regression	75,965	-	-	-	384,871	829,576	-	16,340	-	-
Efermi	Regression	-	145,262	-	-	-	-	-	-	-	-
Exfoliation Energy	Regression	812	-	-	-	-	-	-	-	-	-
Bulk Modulus (Kv)	Regression	23,823	-	-	-	-	-	-	-	-	-
Shear Modulus (Gv)	Regression	23,823	-	-	-	-	-	-	-	-	-
SLME	Regression	9,765	-	-	-	-	-	-	-	-	-
Spillage	Regression	11,377	-	-	-	-	-	-	-	-	-
ϵ_s (OPT)	Regression	52,158	-	-	-	-	-	-	-	-	-
ϵ (DFPT)	Regression	4,704	-	-	-	-	-	-	-	-	-
Max. piezoelectri c strain coeff (dij)	Regression	3,347	-	-	-	-	-	-	-	-	-
Max. piezo. stress coeff (eij)	Regression	4,797	-	-	-	-	-	-	-	-	-
Max. EFG	Regression	11,871	-	-	-	-	-	-	-	-	-
Avg. m_e	Regression	17,643	-	-	-	-	-	-	-	-	-
Is Stable	Classification	-	145,262	-	-	-	-	-	-	-	-
Is Gap Direct	Classification	-	145,262	-	-	-	-	-	-	-	-
n-Seedbeck	Regression	23,211	-	-	-	-	-	-	-	-	-
n-PF	Regression	23,211	-	-	-	-	-	-	-	-	-
p-Seedbeck	Regression	23,211	-	-	-	-	-	-	-	-	-
p-PF	Regression	23,211	-	-	-	-	-	-	-	-	-
Density	Regression	-	145,262	-	-	384,871	-	-	-	-	-
Density Atomic	Regression	-	145,262	-	-	-	-	-	-	-	-
Volume	Regression	-	145,262	-	-	384,871	-	-	-	-	-
Volume Per Atom (VPA)	Regression	-	-	-	-	-	-	84,024	-	-	-
Is Direct	Classification	-	-	10,481	-	-	-	-	-	-	-
Is Direct HSE	Classification	-	-	10,481	-	-	-	-	-	-	-
SOC	Classification	-	-	10,481	-	-	-	-	-	-	-
LCD	Regression	-	-	-	133,524	-	-	-	16,340	-	-
PLD	Regression	-	-	-	133,524	-	-	-	16,340	-	-
Max CO2	Regression	-	-	-	133,524	-	-	-	-	-	-
Min CO2	Regression	-	-	-	133,524	-	-	-	-	-	-
Void Fraction	Regression	-	-	-	133,524	-	-	-	-	-	-
Surface Area m2g	Regression	-	-	-	133,524	-	-	-	-	-	-
Surface Area m2cm3	Regression	-	-	-	133,524	-	-	-	-	-	-

C Chat-like Model Inference Details

Table 8: Hyperparameters used during inference. Temp. represents temperature.

Model Type	Model Name	Input Length	Output Length	Batch Size	Temp.	Top_K
Llama Family	Llama 2-7b-chat-hf	4000	256	256	0.8	10
	Llama 3-8b-Instruct	8000	256	256	0.8	10
	Llama 3.1-8b-Instruct	98000	256	128	0.8	10
	Llama 3.2-3b-Instruct	47000	256	128	0.8	10
Gemma Family	Gemma 7b-it	4000	256	256	0.8	10
	Gemma 1.1-7b-it	4000	256	256	0.8	10
	Gemma 2-9b-it	3000	256	256	0.8	10
Mistral Family	Mistral 7b-Instruct-v0.1	20000	256	256	0.8	10
	Mistral 7b-Instruct-v0.2	20000	256	256	0.8	10
	Mistral 7b-Instruct-v0.3	20000	256	256	0.8	10

D Prompt Templates

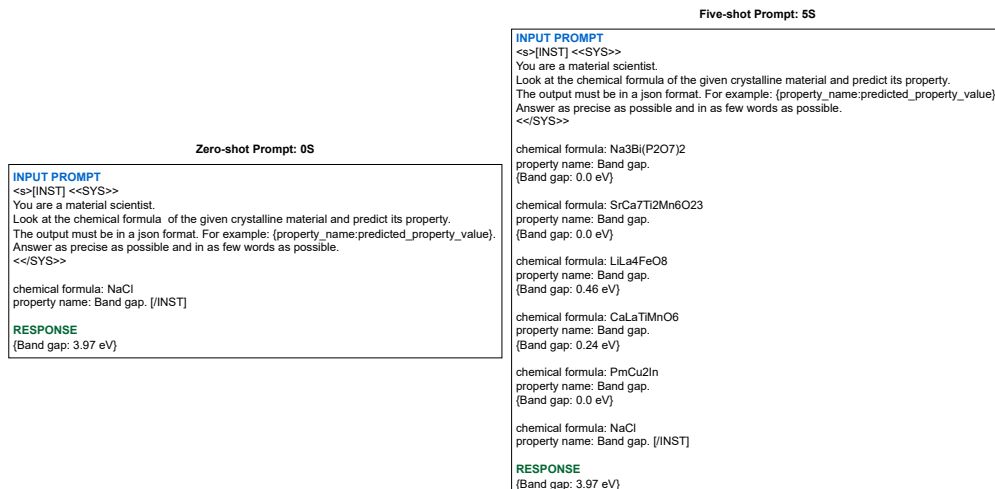


Figure 4: Prompt templates when the input is a chemical formula.

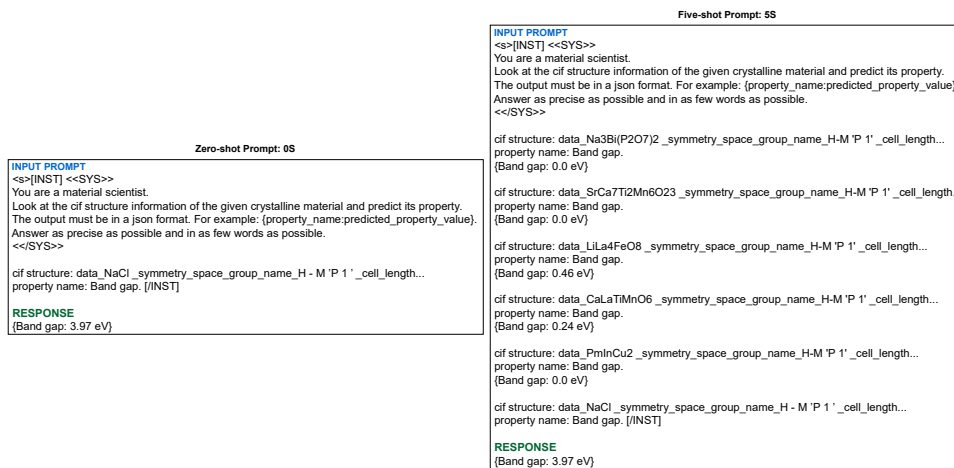


Figure 5: Prompt templates when the input is a CIF file.

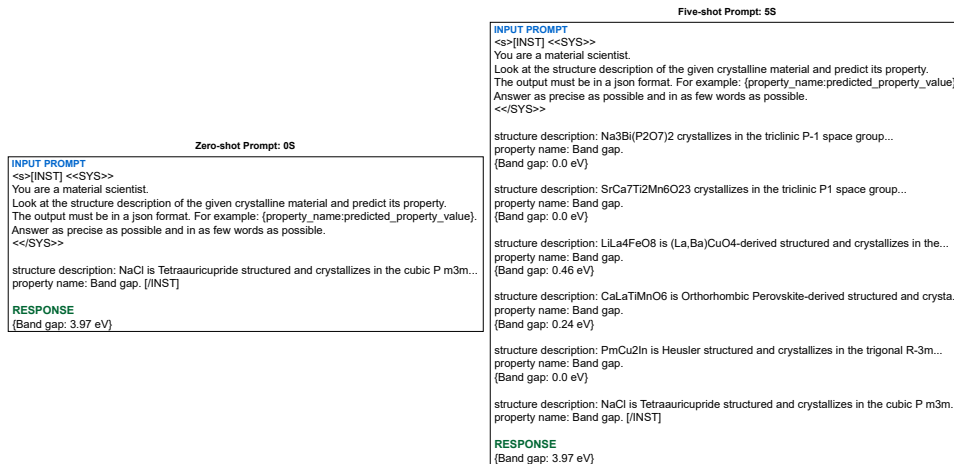


Figure 6: Prompt templates when the input is a crystal structure description.

E Result Details for Each Dataset

E.1 Detailed MAD:MAE Results

Table 9: Results for MP dataset. The performance on regression tasks is evaluated in terms of MAD:MAE ratio (the higher the better) while that of classification tasks (Is Stable and Is Gab Direct) is evaluated in terms of AUC score. FEPA: Formation Energy Per Atom, EPA: Energy Per Atom.

Input	Model	FEPA 145.2K	Bandgap 145.3K	EPA 145.2K	Ehull 145.2K	Efermi 145.2K	Density 145.2K	Density Atomic 145.2K	Volume 145.2K	Is Stable 145.2K	Is Gab Direct 145.2K
CIF	CGCNN (baseline)	8.151	3.255	7.224	3.874	3.689	8.773	5.888	1.703	0.882	0.810
Comp.	Llama 2-7b-chat:0S	0.008	0.623	0.009	0.001	0.003	0.967	0.754	0.747	0.500	0.482
	Llama 2-7b-chat:5S	0.33	1.217	0.239	0.132	0.706	0.899	0.724	0.771	0.502	0.512
	MatBERT-109M	8.151	2.971	9.32	2.583	3.527	7.626	5.26	3.099	0.764	0.681
	LLM-Prop-35M	7.482	2.345	7.437	2.006	3.159	6.682	3.523	2.521	0.746	0.636
CIF	Llama 2-7b-chat:0S	0.032	0.135	0.022	0.001	0.015	0.97	0.549	1.41	0.503	0.499
	Llama 2-7b-chat:5S	Inval.	1.111	0.289	Inval.	0.685	0.98	0.99	0.926	0.498	0.506
	MatBERT-109M	11.017	3.423	13.244	3.808	4.435	10.426	6.686	6.58	0.790	0.710
	LLM-Prop-35M	14.322	3.758	17.354	2.182	4.515	13.834	4.913	7.556	0.776	0.700
Descr.	Llama 2-7b-chat:0S	0.019	0.633	0.023	0.001	0.008	1.31	0.693	0.807	0.500	0.500
	Llama 2-7b-chat:5S	0.394	1.061	0.297	0.247	0.684	0.916	0.782	0.704	0.500	0.504
	MatBERT-109M	11.935	3.524	13.851	4.085	4.323	9.9	6.899	6.693	0.794	0.713
	LLM-Prop-35M	15.913	3.931	18.412	2.74	4.598	14.388	4.063	8.888	0.794	0.690

Table 10: Results for JARVIS-DFT. The performance on regression tasks is evaluated in terms of MAD:MAE ratio (the higher the better). FEPA: Formation Energy Per Atom, Tot. En.: Total Energy, Exf. En.: Exfoliation Energy.

Input	Model	FEPA 75.9K	Bandgap (OPT) 75.9K	Tot. En. 75.9K	Ehull 75.9K	Bandgap (MBJ) 19.8K	Kv 23.8K	Gv 23.8K	SLME 9.7K	Spillage 11.3K	ϵ_x (OPT) 18.2K
CIF	CGCNN (baseline)	13.615	4.797	22.906	1.573	4.497	3.715	2.337	1.862	1.271	2.425
Comp.	Llama 2-7b-chat:0S	0.021	0.011	0.02	0.005	0.92	0.428	0.374	0.148	Inval.	0.18
	Llama 2-7b-chat:5S	0.886	0.011	0.02	1.292	0.979	0.88	0.992	0.456	0.85	1.148
	MatBERT-109M	6.808	4.083	9.21	2.786	3.755	2.906	1.928	1.801	1.243	2.017
	LLM-Prop-35M	4.765	2.621	5.936	2.073	2.922	2.162	1.654	1.575	1.14	1.734
CIF	Llama 2-7b-chat:0S	0.023	0.011	0.02	0.002	0.193	0.278	0.358	0.186	0.702	0.781
	Llama 2-7b-chat:5S	0.859	Inval.	Inval.	1.173	1.054	0.874	0.91	0.486	0.916	1.253
	MatBERT-109M	10.211	5.483	15.673	4.862	5.344	4.283	2.6	2.208	1.444	2.408
	LLM-Prop-35M	12.996	3.331	22.058	2.648	4.93	4.121	2.409	2.175	1.37	2.135
Descr.	Llama 2-7b-chat:0S	0.007	0.011	0.02	0.004	0.94	0.498	0.382	0.07	0.135	0.647
	Llama 2-7b-chat:5S	0.845	0.011	0.02	1.273	1.033	0.87	0.969	0.461	0.857	1.201
	MatBERT-109M	10.211	5.33	15.141	4.691	5.01	4.252	2.623	2.178	1.452	2.384
	LLM-Prop-35M	12.614	3.427	23.509	4.532	4.983	4.128	2.419	2.061	1.307	2.334
		ϵ (DFPT) 4.7K	Max. Piezo. (dij) 3.3K	Max. Piezo. (eij) 4.7K	Max. EFG 11.8K	Exf. En. 0.8K	Avg. m_x 17.6K	n-Seebeck 23.2K	n-PF 23.2K	p-Seebeck 23.2K	p-PF 23.2K
CIF	CGCNN (baseline)	1.12	0.418	1.291	1.787	0.842	1.796	2.23	1.573	3.963	1.59
Comp.	Llama 2-7b-chat:0S	0.012	0.121	0.001	0.141	0.384	0.028	0.874	0.801	0.971	0.874
	Llama 2-7b-chat:5S	1.416	1.289	1.305	0.765	0.512	0.535	1.008	1.04	0.93	0.568
	MatBERT-109M	1.533	1.464	1.426	1.658	1.124	2.093	1.908	1.318	2.752	1.356
	LLM-Prop-35M	1.454	1.447	1.573	1.38	1.042	1.658	1.725	1.145	2.233	1.285
CIF	Llama 2-7b-chat:0S	0.033	0.104	0.001	0.246	0.411	0.041	0.429	0.766	0.83	0.826
	Llama 2-7b-chat:5S	Inval.	Inval.	Inval.	0.796	0.51	Inval.	1.039	1.396	Inval.	Inval.
	MatBERT-109M	1.509	1.758	2.405	2.143	1.374	2.45	2.268	1.446	3.337	1.476
	LLM-Prop-35M	1.578	2.103	2.405	1.936	1.044	1.796	1.955	1.332	2.503	1.399
Descr.	Llama 2-7b-chat:0S	0.08	0.266	0.001	0.138	0.285	0.019	0.769	0.793	0.825	0.829
	Llama 2-7b-chat:5S	1.649	1.174	1.152	0.806	0.661	0.523	1.098	1.024	0.948	0.563
	MatBERT-109M	1.534	1.807	2.556	2.081	1.36	2.597	2.241	1.432	3.26	1.565
	LLM-Prop-35M	1.64	2.116	2.315	1.978	1.168	1.858	2.154	1.364	2.61	1.407

Table 11: Results for SNUMAT. The performance on regression tasks is evaluated in terms of MAD:MAE ratio (the higher the better) while that of classification tasks (Is Direct, Is Direct HSE, and SOC) is evaluated in terms of AUC score.

Input	Model	Bandgap GGA 10.3K	Bandgap HSE 10.3K	Bandgap GGA Optical 10.3K	Bandgap HSE Optical 10.3K	Is Direct 10.3K	Is Direct HSE 10.3K	SOC 10.3K
CIF	CGCNN (baseline)	2.075	2.257	1.727	1.835	0.691	0.675	0.800
Comp.	Llama 2-7b-chat:0S	0.797	0.948	1.156	0.859	0.503	0.484	Inval.
	Llama 2-7b-chat:5S	1.267	1.327	0.862	1.174	0.475	0.468	0.455
	MatBERT-109M	1.899	1.975	1.646	1.793	0.671	0.645	0.820
	LLM-Prop-35M	1.533	1.621	1.392	1.491	0.647	0.624	0.829
CIF	Llama 2-7b-chat:0S	0.346	0.454	1.09	0.838	0.479	0.488	0.500
	Llama 2-7b-chat:5S	Inval.	Inval.	Inval.	Inval.	0.494	0.500	0.427
	MatBERT-109M	2.28	2.472	1.885	1.889	0.677	0.650	0.823
	LLM-Prop-35M	1.23	2.401	1.786	1.9	0.661	0.664	0.656
Descr.	Llama 2-7b-chat:0S	0.802	0.941	1.013	0.779	0.499	0.509	Inval.
	Llama 2-7b-chat:5S	0.774	1.315	0.901	1.172	0.594	0.623	0.486
	MatBERT-109M	2.298	2.433	1.901	1.978	0.683	0.645	0.862
	LLM-Prop-35M	2.251	2.142	1.84	1.569	0.681	0.657	0.866

Table 12: Results for GNoME. The performance on regression tasks is evaluated in terms of MAD:MAE ratio (the higher the better). FEPA: Formation Energy Per Atom, DEPA: Decomposition Energy Per Atom, Tot. En.: Total Energy.

Input	Model	FEPA 376.2K	Bandgap 282.7K	DEPA 376.2K	Tot. En. 282.7K	Volume 282.7K	Density 282.7K
CIF	CGCNN (baseline)	34.57	8.549	2.787	7.443	7.967	56.077
Comp.	Llama 2-7b-chat:0S	0.002	0.177	0.0	0.088	0.455	0.368
	Llama 2-7b-chat:5S	0.194	0.086	0.255	0.765	1.006	0.865
	MatBERT-109M	30.248	4.692	2.787	8.57	13.157	15.145
	LLM-Prop-35M	25.472	3.735	1.858	21.624	16.556	25.615
CIF	Llama 2-7b-chat:0S	0.003	0.045	0.0	0.706	43.331	0.794
	Llama 2-7b-chat:5S	Inval.	0.087	Inval.	Inval.	1.029	0.878
	MatBERT-109M	24.199	9.16	3.716	15.309	16.691	16.467
	LLM-Prop-35M	28.469	3.926	3.344	17.837	17.082	25.615
Descr.	Llama 2-7b-chat:0S	0.002	0.114	0.0	0.661	0.654	0.805
	Llama 2-7b-chat:5S	0.192	0.086	0.106	0.75	1.006	0.891
	MatBERT-109M	30.248	5.829	3.716	18.205	17.824	16.599
	LLM-Prop-35M	28.469	5.27	3.716	17.02	17.02	25.936

Table 13: Results for hMOF. The performance on regression tasks is evaluated in terms of MAD:MAE ratio (the higher the better).

Input	Model	Max CO2 132.7K	Min CO2 132.7K	LCD 132.7K	PLD 132.7K	Void Fraction 132.7K	Surface Area m2g 132.7K	Surface Area m2cm3 132.7K
CIF	CGCNN (baseline)	1.719	1.617	1.989	1.757	2.912	3.765	2.039
Comp.	Llama 2-7b-chat:0S	0.011	0.002	0.009	0.008	0.5	0.454	0.233
	Llama 2-7b-chat:5S	0.679	0.058	0.949	1.026	0.945	0.567	0.366
	MatBERT-109M	1.335	1.41	1.435	1.378	1.57	1.517	1.367
	LLM-Prop-35M	1.41	1.392	1.432	1.468	1.672	1.657	1.321
CIF	Llama 2-7b-chat:0S	0.017	0.003	0.016	0.011	0.549	0.54	0.359
	Llama 2-7b-chat:5S	Inval.	Inval.	0.951	1.067	Inval.	Inval.	Inval.
	MatBERT-109M	1.421	1.428	1.544	1.482	1.641	1.622	1.461
	LLM-Prop-35M	1.564	1.41	1.753	1.435	1.9	1.926	1.374
Descr.	Llama 2-7b-chat:0S	0.129	0.014	0.026	0.006	0.382	0.497	0.299
	Llama 2-7b-chat:5S	0.684	0.058	0.955	1.006	0.931	0.571	0.37
	MatBERT-109M	1.438	1.466	1.602	1.511	1.719	1.697	1.475
	LLM-Prop-35M	1.659	1.486	1.623	1.789	1.736	2.144	1.508

Table 14: Results for Cantor HEA. The performance on regression tasks is evaluated in terms of MAD:MAE ratio (the higher the better). FEPA: Formation Energy Per Atom, EPA:Energy Per Atom, VPA:Volume Per Atom.

Input	Model	FEPA 84.0K	EPA 84.0K	Ehull 84.0K	VPA 84.0K
CIF	CGCNN (baseline)	9.036	49.521	9.697	2.869
Comp.	Llama 2-7b-chat:0S	0.005	0.098	0.003	0.031
	Llama 2-7b-chat:5S	0.896	0.658	0.928	0.986
	MatBERT-109M	3.286	16.17	5.134	2.489
	LLM-Prop-35M	3.286	22.638	5.134	2.543
CIF	Llama 2-7b-chat:0S	0.001	0.084	0.0	0.004
	Llama 2-7b-chat:5S	Inval.	Inval.	Inval.	Inval.
	MatBERT-109M	7.229	17.607	9.187	5.809
	LLM-Prop-35M	8.341	36.015	11.636	6.919
Descr.	Llama 2-7b-chat:0S	0.001	0.101	0.164	0.011
	Llama 2-7b-chat:5S	0.797	0.615	0.938	0.93
	MatBERT-109M	7.229	17.607	9.187	5.881
	LLM-Prop-35M	8.341	36.015	11.636	7.713

Table 15: Results for QMOF. The performance on regression tasks is evaluated in terms of MAD:MAE ratio (the higher the better). Tot. En.: Total Energy.

Input	Model	Bandgap 7.6K	Tot. En. 7.6K	LCD 7.6K	PLD 7.6K
CIF	CGCNN (baseline)	2.431	1.489	4.068	4.317
Comp.	Llama 2-7b-chat:0S	0.901	0.26	0.045	0.009
	Llama 2-7b-chat:5S	0.648	0.754	1.241	1.086
	MatBERT-109M	1.823	1.695	2.329	2.349
	LLM-Prop-35M	1.759	1.621	2.293	2.157
CIF	Llama 2-7b-chat:0S	0.201	0.244	0.02	0.011
	Llama 2-7b-chat:5S	Inval.	Inval.	Inval.	Inval.
	MatBERT-109M	1.994	4.378	2.908	2.818
	LLM-Prop-35M	2.166	4.323	2.947	2.87
Descr.	Llama 2-7b-chat:0S	0.358	0.217	0.025	0.006
	Llama 2-7b-chat:5S	0.777	0.713	1.125	1.17
	MatBERT-109M	2.166	4.133	2.981	2.941
	LLM-Prop-35M	2.091	4.312	2.831	2.829

Table 16: Results for JARVIS-QETB. The performance on regression tasks is evaluated in terms of MAD:MAE ratio (the higher the better). FEPA: Formation Energy Per Atom, EPA:Energy Per Atom, Tot. En.: Total Energy, Ind. Bandgap: Indirect Bandgap.

Input	Model	FEPA 623.9K	EPA 623.9K	Tot. En. 623.9K	Ind. Bandgap 623.9K
CIF	CGCNN (baseline)	1.964	228.201	11.218	5.534
Comp.	Llama 2-7b-chat:0S	0.003	0.369	0.172	0.21
	Llama 2-7b-chat:5S	0.812	1.037	1.032	1.306
	MatBERT-109M	1.431	37.979	8.19	0.21
	LLM-Prop-35M	2.846	211.757	21.309	1.861
CIF	Llama 2-7b-chat:0S	0.003	0.412	0.656	0.04
	Llama 2-7b-chat:5S	0.8	1.024	1.076	1.71
	MatBERT-109M	24.72	135.156	26.094	4.779
	LLM-Prop-35M	23.346	318.291	48.192	1.845
Descr.	Llama 2-7b-chat:0S	0.003	0.408	0.484	0.16
	Llama 2-7b-chat:5S	0.85	1.015	1.035	1.021
	MatBERT-109M	26.265	122.884	29.409	7.788
	LLM-Prop-35M	22.513	312.218	35.43	1.845

Table 17: Results for OQMD. The performance on regression tasks is evaluated in terms of MAD:MAE ratio (the higher the better). FEPA: Formation Energy Per Atom.

Input	Model	FEPA 963.5K	Bandgap 963.5K
CIF	CGCNN (baseline)	22.291	6.701
Comp.	Llama 2-7b-chat:0S	0.019	0.192
	Llama 2-7b-chat:5S	1.013	1.306
	MatBERT-109M	7.662	3.883
	LLM-Prop-35M	9.195	2.845
CIF	Llama 2-7b-chat:0S	0.009	0.047
	Llama 2-7b-chat:5S	1.051	1.731
	MatBERT-109M	13.879	7.163
	LLM-Prop-35M	18.861	3.22
Descr.	Llama 2-7b-chat:0S	0.025	0.187
	Llama 2-7b-chat:5S	0.991	1.468
	MatBERT-109M	15.012	7.041
	LLM-Prop-35M	16.346	3.644

Table 18: Results for OMDB. The performance on regression tasks is evaluated in terms of MAD:MAE ratio (the higher the better).

Input	Model	Bandgap 12.1K
CIF	CGCNN (baseline)	2.751
Comp.	Llama 2-7b-chat:0S	0.886
	Llama 2-7b-chat:5S	1.009
	MatBERT-109M	1.554
	LLM-Prop-35M	1.507
CIF	Llama 2-7b-chat:0S	0.159
	Llama 2-7b-chat:5S	0.930
	MatBERT-109M	1.777
	LLM-Prop-35M	1.777
Descr.	Llama 2-7b-chat:0S	0.155
	Llama 2-7b-chat:5S	1.002
	MatBERT-109M	1.847
	LLM-Prop-35M	1.656

E.2 Detailed MAE Results

Table 19: Results for Materials Project (MP). The ↓ and ↑ on the right of each property denote the MAE error and AUC score, respectively. The Dummy model represents the MAD score that is calculated on the ground truth of each property.

Input	Model	FEPA ↓	Bandgap ↓	EPA ↓	Ehull ↓	Efermi ↓	Density ↓	Density atomic ↓	Volume ↓	Is stable ↑	Is gab direct ↑	Wtd. Avg. (MAD/MAE) ↑	Wtd. Avg. AUC ↑
-	Dummy (MAD)	1.003	1.191	1.51	0.225	2.239	2.158	11.693	342.606	-	-	-	-
Structure	CGCNN (baseline)	0.123	0.366	0.209	0.058	0.607	0.246	1.986	201.186	0.882	0.810	5.319	0.846
Composition	Llama 2-7b-chat:0S	128.007	1.913	163.899	195.908	673.939	2.231	15.503	458.456	0.500	0.482	0.389	0.491
	Llama 2-7b-chat:5S	3.034	0.979	6.330	1.706	3.172	2.400	16.150	444.378	0.502	0.512	0.627	0.507
	MatBERT-109M	0.123	0.401	0.162	0.087	0.635	0.283	2.223	110.556	0.764	0.681	5.316	0.722
	LLM-Prop-35M	0.134	0.508	0.203	0.112	0.709	0.323	3.319	135.924	0.746	0.636	4.364	0.691
Structure	Llama 2-7b-chat:0S	31.515	8.819	69.840	213.547	148.541	2.224	21.296	243.050	0.503	0.499	0.392	0.501
	Llama 2-7b-chat:5S	Inval.	1.072	5.219	Inval.	3.268	2.203	11.806	370.160	0.498	0.506	Inval.	0.502
	MatBERT-109M	0.091	0.348	0.114	0.059	0.505	0.207	1.749	52.068	0.790	0.710	7.452	0.750
	LLM-Prop-35M	0.070	0.317	0.087	0.103	0.496	0.156	2.380	45.340	0.776	0.700	8.554	0.738
Description	Llama 2-7b-chat:0S	53.083	1.881	66.971	313.255	288.275	1.647	16.874	424.737	0.500	0.500	0.437	0.500
	Llama 2-7b-chat:5S	2.544	1.123	5.087	0.910	3.274	2.356	14.961	486.650	0.500	0.504	0.635	0.502
	MatBERT-109M	0.084	0.338	0.109	0.055	0.518	0.218	1.695	51.189	0.794	0.713	7.651	0.735
	LLM-Prop-35M	0.063	0.303	0.082	0.082	0.487	0.150	2.878	38.548	0.794	0.690	9.116	0.742

Table 20: Results for JARVIS-DFT. The ↓ on the right of each property denotes the MAE error.

Input	Model	FEPA ↓	Bandgap (OPT) ↓	Total energy ↓	Ehull ↓	Bandgap (MRJ) ↓	Kv ↓	Gv ↓	SLME ↓	Spillage ↓	ϵ_e (OPT) ↓	Wtd. Avg. (MAD/MAE) ↑
-	Dummy (MAD)	0.858	0.959	1.787	0.267	1.844	53.762	27.455	10.538	0.508	65.886	-
Structure	CGCNN (baseline)	0.063	0.200	0.078	0.170	0.410	14.470	11.750	5.660	0.400	27.170	7.048
Composition	Llama 2-7b-chat:0S	40.722	86.989	91.114	53.109	2.005	125.545	73.335	71.208	Inval.	365.525	Inval.
	Llama 2-7b-chat:5S	0.968	87.324	90.542	0.207	1.883	61.121	27.672	23.093	0.598	57.394	0.704
	MatBERT-109M	0.126	0.235	0.194	0.096	0.491	18.498	14.241	5.851	0.409	32.661	4.103
	LLM-Prop-35M	0.180	0.366	0.301	0.129	0.631	24.868	16.603	6.689	0.446	37.993	2.912
Structure	Llama 2-7b-chat:0S	37.893	86.424	90.286	135.879	9.532	193.714	76.784	56.666	0.724	84.332	0.216
	Llama 2-7b-chat:5S	0.999	Inval.	Inval.	0.228	1.749	61.509	30.156	21.678	0.555	52.576	Inval.
	MatBERT-109M	0.084	0.175	0.114	0.055	0.345	12.553	10.560	4.772	0.352	27.364	6.211
	LLM-Prop-35M	0.066	0.288	0.081	0.101	0.374	13.046	11.399	4.845	0.371	30.867	6.756
Description	Llama 2-7b-chat:0S	117.691	87.327	90.615	72.709	1.962	108.062	71.895	150.412	3.753	101.906	0.247
	Llama 2-7b-chat:5S	1.015	87.323	89.595	0.210	1.784	61.783	28.345	22.857	0.593	54.850	0.703
	MatBERT-109M	0.084	0.180	0.118	0.057	0.368	12.645	10.466	4.839	0.350	27.633	6.083
	LLM-Prop-35M	0.068	0.280	0.076	0.059	0.370	13.023	11.352	5.113	0.389	28.231	7.204
-	Dummy (MAD)	43.451	14.525	0.245	44.129	42.08	0.216	111.33	695.882	168.11	699.799	-
Structure	CGCNN (baseline)	38.780	34.710	0.190	24.700	50.000	0.120	49.920	442.300	42.420	440.26	7.048
Composition	Llama 2-7b-chat:0S	3626.217	120.287	228.849	312.490	109.464	7.708	127.267	868.257	173.183	800.024	Inval.
	Llama 2-7b-chat:5S	30.680	11.272	0.188	57.654	82.128	0.403	110.485	669.338	180.679	1231.228	0.704
	MatBERT-109M	28.340	9.920	0.172	26.621	37.445	0.103	58.342	528.070	61.085	516.190	4.103
	LLM-Prop-35M	29.881	10.037	0.156	31.966	40.385	0.130	64.538	608.007	75.268	544.737	2.912
Structure	Llama 2-7b-chat:0S	1317.680	139.160	196.532	179.067	102.276	5.254	259.753	908.067	202.459	847.011	0.216
	Llama 2-7b-chat:5S	Inval.	Inval.	Inval.	55.417	82.580	Inval.	107.189	498.324	Inval.	Inval.	Inval.
	MatBERT-109M	28.789	8.262	0.102	20.593	30.623	0.313	49.096	481.132	50.382	474.278	6.211
	LLM-Prop-35M	27.529	6.908	0.102	22.791	40.324	0.120	56.953	522.337	67.153	500.348	6.756
Description	Llama 2-7b-chat:0S	543.798	54.605	273.968	320.801	147.706	11.616	144.830	877.009	203.677	843.939	0.247
	Llama 2-7b-chat:5S	26.354	12.374	0.213	54.739	63.690	0.412	101.373	679.530	177.250	1242.988	0.703
	MatBERT-109M	28.329	8.036	0.096	21.202	30.948	0.083	49.674	486.017	51.570	447.099	6.083
	LLM-Prop-35M	26.491	6.863	0.106	22.308	36.031	0.116	51.686	510.280	64.402	497.515	7.204

Table 21: Results for SNUMAT. The ↓ and ↑ on the right of each property denote the MAE error and AUC score, respectively.

Input	Model	Bandgap GGA ↓	Bandgap HSE ↓	Bandgap GGA optical ↓	Bandgap HSE optical ↓	Is direct ↑	Is direct HSE ↑	SOC ↑	Wtd. Avg. (MAD/MAE) ↑	Wtd. Avg. AUC ↑
-	Dummy (MAD)	0.875	1.092	1.154	1.343	-	-	-	-	-
Structure	CGCNN (baseline)	0.422	0.484	0.668	0.732	0.691	0.675	0.800	1.973	0.722
Composition	Llama 2-7b-chat:0S	1.999	1.152	0.998	1.564	0.503	0.484	Inval.	0.940	Inval.
	Llama 2-7b-chat:5S	0.691	0.823	1.339	1.144	0.475	0.468	0.455	1.157	0.466
	MatBERT-109M	0.461	0.553	0.701	0.749	0.671	0.645	0.820	1.828	0.712
	LLM-Prop-35M	0.571	0.674	0.829	0.901	0.647	0.624	0.829	1.509	0.716
Structure	Llama 2-7b-chat:0S	2.531	2.405	1.058	1.603	0.479	0.488	0.500	0.682	0.489
	Llama 2-7b-chat:5S	Inval.	Inval.	Inval.	Inval.	0.494	0.500	0.427	Inval.	0.474
	MatBERT-109M	0.384	0.442	0.612	0.711	0.677	0.650	0.823	2.131	0.717
	LLM-Prop-35M	0.712	0.455	0.646	0.707	0.661	0.664	0.656	1.829	0.660
Description	Llama 2-7b-chat:0S	1.992	1.161	1.139	1.725	0.499	0.509	Inval.	0.883	Inval.
	Llama 2-7b-chat:5S	1.131	0.831	1.281	1.146	0.594	0.623	0.486	1.040	0.568
	MatBERT-109M	0.381	0.449	0.607	0.679	0.683	0.645	0.862	2.152	0.730
	LLM-Prop-35M	0.389	0.510	0.627	0.856	0.681	0.657	0.866	1.950	0.735

Table 22: Results for GNoME. The ↓ on the right of each property denotes the MAE error.

Input	Model	FEPA ↓	Bandgap ↓	DEPA ↓	Total energy ↓	Volume ↓	Density ↓	Wtd. Avg. (MAD/MAE) ↑
-	Dummy (MAD)	0.484	0.385	0.033	62.752	193.386	2.075	-
Structure	CGCNN (baseline)	0.014	0.045	0.012	8.431	24.274	0.037	19.478
Composition	Llama 2-7b-chat:0S	251.420	2.170	233.95	713.047	425.052	5.633	0.164
	Llama 2-7b-chat:5S	2.494	4.471	0.131	81.987	192.289	2.398	0.499
	MatBERT-109M	0.016	0.082	0.012	7.322	14.698	0.137	12.834
	LLM-Prop-35M	0.019	0.103	0.018	2.902	11.681	0.081	15.599
Structure	Llama 2-7b-chat:0S	150.755	8.481	77.790	88.822	4.463	2.612	6.746
	Llama 2-7b-chat:5S	Inval.	4.418	Inval.	Inval.	188.008	2.364	Inval.
	MatBERT-109M	0.020	0.042	0.009	4.099	11.586	0.126	14.227
	LLM-Prop-35M	0.017	0.098	0.010	3.518	11.321	0.081	16.032
Description	Llama 2-7b-chat:0S	259.528	3.360	311.944	94.968	295.904	2.576	0.336
	Llama 2-7b-chat:5S	2.524	4.457	0.315	83.714	192.259	2.328	0.470
	MatBERT-109M	0.016	0.066	0.009	3.447	10.850	0.125	15.558
	LLM-Prop-35M	0.017	0.073	0.009	3.687	11.362	0.080	16.224

Table 23: Results for hMOF. The ↓ on the right of each property denotes the MAE error.

Input	Model	Max CO2 ↓	Min CO2 ↓	LCD ↓	PLD ↓	Void fraction ↓	Surface area m2g ↓	Surface area m2cm3 ↓	Wtd. Avg. (MAD/MAE) ↑
-	Dummy (MAD)	2.245	0.11	3.506	3.59	0.181	1469.493	604.098	-
Structure	CGCNN (baseline)	1.306	0.068	1.763	2.043	0.062	390.269	296.248	2.257
Composition	Llama 2-7b-chat:0S	199.955	60.032	381.040	447.976	0.361	3239.754	2593.456	0.174
	Llama 2-7b-chat:5S	3.305	1.902	3.696	3.500	0.191	2592.529	1651.846	0.655
	MatBERT-109M	1.682	0.078	2.443	2.606	0.115	968.706	441.879	1.430
	LLM-Prop-35M	1.592	0.079	2.449	2.445	0.108	886.750	457.435	1.479
Structure	Llama 2-7b-chat:0S	128.932	32.271	221.708	327.567	0.329	2721.352	1682.345	0.214
	Llama 2-7b-chat:5S	Inval.	Inval.	3.688	3.365	Inval.	Inval.	Inval.	Inval.
	MatBERT-109M	1.580	0.077	2.271	2.423	0.110	906.251	413.508	1.514
	LLM-Prop-35M	1.435	0.078	2.000	2.501	0.095	763.111	439.739	1.623
Description	Llama 2-7b-chat:0S	17.457	7.884	134.936	572.296	0.472	2956.530	2019.484	0.193
	Llama 2-7b-chat:5S	3.281	1.891	3.671	3.568	0.194	2571.702	1634.674	0.653
	MatBERT-109M	1.561	0.075	2.189	2.376	0.105	865.712	409.503	1.558
	LLM-Prop-35M	1.353	0.074	2.160	2.007	0.104	685.379	400.681	1.706

Table 24: Results for Cantor HEA. The ↓ on the right of each property denotes the MAE error.

Input	Model	FEPA ↓	EPA ↓	Ehull ↓	VPA ↓	Wtd. Avg. (MAD/MAE) ↑
-	Dummy (MAD)	0.108	0.792	0.175	0.470	-
Structure	CGCNN (baseline)	0.012	0.016	0.018	0.164	17.780
Composition	Llama 2-7b-chat:0S	21.986	8.097	61.275	15.079	0.034
	Llama 2-7b-chat:5S	0.121	1.205	0.188	0.477	0.867
	MatBERT-109M	0.033	0.049	0.034	0.189	6.769
	LLM-Prop-35M	0.033	0.035	0.034	0.185	8.400
Structure	Llama 2-7b-chat:0S	141.784	9.483	2791.970	107.467	0.022
	Llama 2-7b-chat:5S	Inval.	Inval.	Inval.	Inval.	Inval.
	MatBERT-109M	0.015	0.045	0.019	0.081	9.958
	LLM-Prop-35M	0.013	0.022	0.015	0.068	15.728
Description	Llama 2-7b-chat:0S	212.607	7.843	1.062	44.740	0.069
	Llama 2-7b-chat:5S	0.136	1.289	0.186	0.506	0.820
	MatBERT-109M	0.015	0.045	0.019	0.080	9.976
	LLM-Prop-35M	0.013	0.022	0.015	0.061	15.926

Table 25: Results for QMOF. The ↓ on the right of each property denotes the MAE error.

Input	Model	Bandgap ↓	Total energy ↓	LCD ↓	PLD ↓	Wtd. Avg. (MAD/MAE) ↑
-	Dummy (MAD)	0.853	389.53	3.926	3.432	-
Structure	CGCNN (baseline)	0.351	261.601	0.965	0.795	3.076
Composition	Llama 2-7b-chat:0S	0.947	1498.974	87.894	395.609	0.303
	Llama 2-7b-chat:5S	1.316	516.724	3.163	3.161	0.932
	MatBERT-109M	0.468	229.838	1.686	1.461	2.049
	LLM-Prop-35M	0.485	240.310	1.712	1.591	1.958
Structure	Llama 2-7b-chat:0S	4.249	1598.672	191.713	323.684	0.119
	Llama 2-7b-chat:5S	Inval.	Inval.	Inval.	Inval.	Inval.
	MatBERT-109M	0.428	88.984	1.350	1.218	3.024
	LLM-Prop-35M	0.394	90.098	1.332	1.196	3.076
Description	Llama 2-7b-chat:0S	2.384	1791.591	154.422	539.926	0.152
	Llama 2-7b-chat:5S	1.098	546.695	3.491	2.933	0.946
	MatBERT-109M	0.394	94.257	1.317	1.167	3.055
	LLM-Prop-35M	0.408	90.342	1.387	1.213	3.016

Table 26: Results for JARVIS-QETB. The ↓ on the right of each property denotes the MAE error.

Input	Model	FEPA ↓	EPA ↓	Total energy ↓	Indirect Bandgap ↓	Wtd. Avg. (MAD/MAE) ↑
-	Dummy (MAD)	1.261	719.975	88.432	0.210	-
Structure	CGCNN (baseline)	0.642	3.155	7.883	0.038	61.729
Composition	Llama 2-7b-chat:0S	438.919	1949.724	514.448	1.000	0.188
	Llama 2-7b-chat:5S	1.553	694.574	85.674	0.161	1.047
	MatBERT-109M	0.881	18.957	10.798	1.000	11.952
	LLM-Prop-35M	0.443	3.400	4.150	0.113	59.443
Structure	Llama 2-7b-chat:0S	489.087	1746.612	134.783	5.319	0.278
	Llama 2-7b-chat:5S	1.576	703.03	82.224	0.123	1.152
	MatBERT-109M	0.051	5.327	3.389	0.044	47.687
	LLM-Prop-35M	0.054	2.262	1.835	0.114	97.919
Description	Llama 2-7b-chat:0S	446.254	1763.805	182.817	1.316	0.264
	Llama 2-7b-chat:5S	1.484	709.001	85.454	0.206	0.980
	MatBERT-109M	0.048	5.859	3.007	0.027	46.586
	LLM-Prop-35M	0.056	2.306	2.496	0.114	93.001

Table 27: Results for OQMD. The ↓ on the right of each property denotes the MAE error.

Input	Model	FEPA ↓	Bandgap ↓	Wtd. Avg. (MAD/MAE) ↑
-	Dummy (MAD)	0.736	0.415	-
Structure	CGCNN (baseline)	0.033	0.062	14.496
Composition	Llama 2-7b-chat:0S	38.194	2.166	0.105
	Llama 2-7b-chat:5S	0.726	0.318	1.160
	MatBERT-109M	0.096	0.107	5.772
	LLM-Prop-35M	0.080	0.146	6.020
Structure	Llama 2-7b-chat:0S	80.815	8.767	0.028
	Llama 2-7b-chat:5S	0.700	0.240	1.391
	MatBERT-109M	0.053	0.058	10.521
	LLM-Prop-35M	0.039	0.129	11.041
Description	Llama 2-7b-chat:0S	29.677	2.221	0.106
	Llama 2-7b-chat:5S	0.742	0.283	1.230
	MatBERT-109M	0.049	0.059	11.027
	LLM-Prop-35M	0.045	0.114	9.995

Table 28: Results for OMDB. The ↓ on the right of each property denotes the MAE error.

Input	Model	Bandgap ↓	MAD/MAE ↑
-	Dummy (MAD)	0.803	-
Structure	CGCNN (baseline)	0.292	2.751
Composition	Llama 2-7b-chat:0S	0.907	0.885
	Llama 2-7b-chat:5S	0.796	1.009
	MatBERT-109M	0.517	1.554
	LLM-Prop-35M	0.533	1.507
Structure	Llama 2-7b-chat:0S	5.051	0.159
	Llama 2-7b-chat:5S	0.864	0.930
	MatBERT-109M	0.452	1.777
	LLM-Prop-35M	0.452	1.777
Description	Llama 2-7b-chat:0S	5.194	0.155
	Llama 2-7b-chat:5S	0.802	1.001
	MatBERT-109M	0.435	1.847
	LLM-Prop-35M	0.485	1.656